TSINGHUA SCIENCE AND TECHNOLOGY
ISSN 1007-0214 09/16 pp324-331
Volume 11, Number 3, June 2006

Application of Method-of-Lines to Charging-Up Process in Pipelines with Entrapped Air*

ZHANG Yongliang (张永良)**, K. Vairavamoorthy†

**State Key Laboratory of Hydroscience and Hydraulic Engineering,
Department of Hydraulic Engineering, Tsinghua University, Beijing 100084, China;
† Department of Civil and Building Engineering, Loughborough University, Leicestershire LE11 3TU, UK**

Abstract: A mathematical model is presented for the charging-up process in an air-entrapped pipeline with moving boundary conditions. A coordinate transformation technique is employed to reduce fluid motion in time-dependent domains to ones in time-independent domains. The nonlinear hyperbolic partial differential equations governing the unsteady motion of fluid combined with an equation for transient shear stress between the pipe wall and the flowing fluid are solved by the method of lines. Results show that ignoring elastic effects overestimates the maximum pressure and underestimates the maximum front velocity of filling fluid. The peak pressure of the entrapped air is sensitive to the length of the initial entrapped air pocket.

Key words: transient flow; charging-up process; pipelines; entrapped air; method of lines

Introduction

The initial charging-up process is an important operation in an intermittent, undulating pipeline system. Recently, the charging-up process has received attention with the aim of predicting the effective duration of supply in different regions of the system[1]. Air pockets collect at high points of an intermittent system when the flow is off. Entrapped air may play a dual role in increasing or decreasing pressure when supply resumes[2]. The behavior of entrapped air has been extensively analyzed using lumped-parameter models[3-7].

Transient flow in rapidly filling pipelines with entrapped air involves the solution of the nonlinear hyperbolic partial differential equations that govern the motion of filling and blocking fluids in a time-varying computational domain. Pressure-wave transmission within the entrapped air region is first quantitatively examined through the method of characteristics solution of these equations by Chaiko and Brinckman[2]. The maximum pressure resulting from the rapid pressurization of a closed system with entrapped air is much higher than ones in a purely liquid system due to compression of the air as it seizes the momentum of the moving fluid. The study is extended to an improved model by incorporating the influence of transient shear stress between the pipe wall and the fluid[8]; the model equations are solved also using the method of characteristics (MOC). The results revealed that transient shear stresses have the potential to change the maximum pressures deduced from a quasi-steady shear stress model, and that the lumped-parameter model overestimates maximum pressures.

In spite of the fact that MOC is the most common approach for hyperbolic water hammer equations, it is inconvenient for problems where a lumped-parameter system of ordinary differential equations (ODEs) in

Received: 2005-01-12; revised: 2005-06-15
* Supported by Program for New Century Excellent Talents in University (No. NCET-04-0093) and the National Natural Science Foundation of China (No. 50539070)
** To whom correspondence should be addressed.
E-mail: yongliangzhang@tsinghua.edu.cn
Tel: 86-10-62797081, Fax: 86-10-62782159

time is required[9]. The method of lines (MOL) provides an appropriate alternative to exploring transient flow behavior for rapidly filling pipelines with entrapped air. This method is a well-established technique, particularly for parabolic transient problems even with shock-like-structures[10,11]. To the authors' knowledge, no work has been devoted to hyperbolic transient pipe flow problems with entrapped air using the MOL, even though many common physical problems are described by first order hyperbolic partial differential equations (PDEs) subject to moving boundaries, such as water hammer equations coupled to kinematic equations for moving fluid-gas interfaces and uniform gas compression equations. A previous study showed that the solution of transient laminar pipe flow problems using the MOL is better than the finite difference method (FDM) with respect to CPU time and its flexibility for incorporation of other conservative equations, particularly for higher Reynolds numbers[12]. Limitation of all these studies lies in solving transient flow problems using the MOL in the time-independent domains where air pockets are absent in pipelines.

This paper is to extend the previous methods of lines for single phase fluid flow with time-independent domains[13] by considering multiphase flow with moving boundaries, and to offer an alternative solution procedure for investigating the problem of transient pipe flow with entrapped air. The presence of two or more entrapped air pockets does not significantly influence the maximum pressure of the first air pocket[6]. Therefore, this paper is limited to the charging-up process in pipelines with one entrapped air pocket. By the water hammer equations, introducing coordinate transformation and then employing the MOL, a general numerical formulation has been established which is capable of analyzing the hydrodynamic problem of adjoining liquid and air regions with time-varying domains, and exploring the effect of entrapped air on transient flow behavior.

1 Mathematical Model

Consider the charging-up process in an undulating pipeline with an entrapped air pocket between filling and blocking fluid columns occupying regions $\Omega_\mathrm{f}=[0,s_\mathrm{f}]$ and $\Omega_\mathrm{b}=[s_\mathrm{b},L_\mathrm{b}+s_\mathrm{b}]$, in which s_f and s_b denote the positions of filling fluid-entrapped air and blocking fluid-entrapped air interfaces. L_b is the blocking fluid column length. A discharge valve positioned upstream is opened and the resultant flow is induced by negative pressure gradients, followed by decompressing the entrapped air and consequently driving blocking fluid to flow downstream. This charging-up process is formulated one-dimensionally, as shown in Fig. 1.

Motion of incompressible fluid is described by the

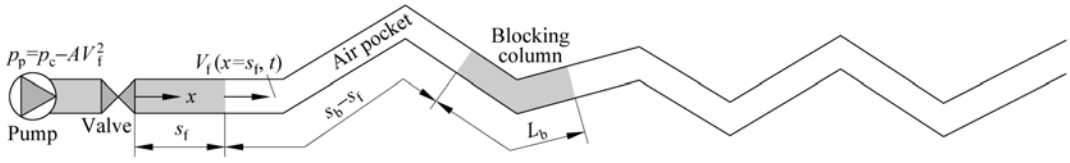

Fig. 1 Schematic of the charging-up process in a pipeline with an entrapped air pocket

velocity $v_k(x,t)$ and pressure $p_k(x,t)$ in which $k=\mathrm{f},\mathrm{b}$ represents the filling and blocking liquids. Uniform expansion and compression of the gas is described by the pressure $p_\mathrm{g}(t)$; t and x denote the time and the distance along the pipeline with its origin coincident with that of the valve. The pump head described by the Suter curve is $p_\mathrm{p}=p_\mathrm{c}-AV_\mathrm{f}^2$, in which A is the pump discharge head parameter. It is assumed that the pipe remains full so that there is a liquid column with a well defined front. Shear stress (τ) between the pipe wall and the filling fluid will consist of steady and unsteady shear stress components, i.e., $\tau=\tau_\mathrm{steady}+\tau_\mathrm{unsteady}$, and given by Refs. [14-17] as follows.

$$\tau_\mathrm{steady}=\frac{1}{8}\rho f v_k|v_k| \tag{1a}$$

$$\tau_\mathrm{unsteady}=\frac{1}{4}\delta\rho D\left[\frac{\partial v_k}{\partial t}+a\,\mathrm{sign}(v_k)\frac{\partial v_k}{\partial x}\right] \tag{1b}$$

where τ_steady and τ_unsteady are the steady and unsteady shear stress components; ρ is the fluid density; D is the internal diameter of the pipe; a is the fluid wave speed in the pipe; f is the Darcy-Weisbach friction coefficient; δ represents the positive relaxation time (transient friction coefficient) and is associated with shear decay

coefficient (C) and Reynolds number (Re),

$$\delta = C^{0.5}, \quad C = \begin{cases} 0.0476 & \text{for laminar flow} \\ 7.41/Re^{\lg(14.3/Re^{0.05})} & \text{for turbulent flow} \end{cases} \tag{1c}$$

which provides a good representation of the friction coefficient for laminar and low Reynolds number transient flow[18]. Therefore, it is reasonable to adopt the above equations to model transient wall shear stress to explore its influence on flow behavior. It should be pointed out that the reason that Eq. (1b) is adopted in this work is given in detail in a previous paper[13].

The motion of fluid governed by the equation of continuity for one-dimensional unsteady flow in the pipeline is[12]

$$\frac{\partial p_k}{\partial t} + v_k \frac{\partial p_k}{\partial x} + \rho a^2 \frac{\partial v_k}{\partial x} = 0, \text{ on } \Omega_k \tag{2}$$

and the equation of momentum is

$$\frac{\partial v_k}{\partial t} + \frac{v_k + a\delta \operatorname{sign}(v_k)}{1+\delta}\frac{\partial v_k}{\partial x} + \frac{1}{(1+\delta)\rho}\frac{\partial p_k}{\partial x} + \frac{f}{2(1+\delta)D} v_k |v_k| + \frac{g}{1+\delta}\frac{\partial h_k}{\partial x} = 0, \text{ on } \Omega_k \tag{3}$$

where h_b and h_f are the elevations of the blocking and filling liquids.

In the entrapped air region between the filling and blocking fluids, an ideal gas is governed by

$$p_g (s_b - s_f)^n = p_{g0} (s_{b0} - s_{f0})^n, \quad \text{on } x \in [s_f, s_b] \tag{4}$$

where p_{g0} is the initial entrapped air pressure; n is the polytropic coefficient, usually 1.2 to 1.4; s_{f0} and s_{b0} are the initial positions of the filling fluid-entrapped air and blocking fluid-entrapped air interfaces.

Equations (2)-(4) are solved subject to boundary conditions. The boundary conditions at the upstream and downstream ends are

$$p_f(x=0,t) = p_{up}, \quad p_b(x = s_b + L_b, t) = p_{down} \tag{5}$$

Matching conditions for pressure at the filling fluid-entrapped air and blocking fluid-entrapped air interfaces are

$$p_f(x = s_f, t) = p_g(t), \quad p_b(x = s_b, t) = p_g(t) \tag{6}$$

and kinematic conditions for these two fluid-gas interfaces are

$$\dot{s}_f(t) = V_f(x = s_f, t), \quad \dot{s}_b(t) = V_b(x = s_b, t),$$
$$\dot{L}_b(t) = V_b(x = s_b + L_b, t) - V_b(x = s_b, t) \tag{7}$$

where p_{up} and p_{down} are the upstream and downstream pressures; the dot over the variables is the material derivative with respect to time.

Introducing two dimensionless coordinates ξ_f and ξ_b,

$$\xi_f = \frac{x}{s_f}, \quad \xi_b = \frac{x - s_b}{L_b} \tag{8}$$

The hydrodynamic problem of adjoining liquid and air regions with time-varying domains can be solved. Upon transforming coordinates, the charging-up process governed by Eqs. (2)-(4) can be rewritten in a compact form,

$$\frac{\partial \boldsymbol{u}_k}{\partial t} + \boldsymbol{b}_k \frac{\partial \boldsymbol{u}_k}{\partial \xi_k} + \boldsymbol{f}_k = \boldsymbol{0}, \quad k = \mathrm{f}, \mathrm{b} \tag{9}$$

with

$$\boldsymbol{u}_f = \begin{Bmatrix} P_f \\ V_f \end{Bmatrix}, \quad \boldsymbol{u}_b = \begin{Bmatrix} P_b \\ V_b \end{Bmatrix},$$

$$\boldsymbol{b}_f = \begin{bmatrix} \dfrac{V_f - \xi_f \dot{s}_f}{s_f} & \dfrac{\rho a^2}{s_f} \\ \dfrac{1}{(1+\delta)\rho s_f} & \dfrac{V_f + a\delta \operatorname{sign}(V_f) - \xi_f \dot{s}_f}{(1+\delta)s_f} \end{bmatrix} \tag{10a}$$

$$\boldsymbol{b}_b = \begin{bmatrix} \dfrac{V_b - (\xi_b \dot{L}_b + \dot{s}_b)}{L_b} & \dfrac{\rho a^2}{L_b} \\ \dfrac{\eta}{(1+\delta)\rho L_b} & \dfrac{V_b + a\delta \operatorname{sign}(V_b) - (\xi_b \dot{L}_b + \dot{s}_b)}{(1+\delta)L_b} \end{bmatrix} \tag{10b}$$

$$\boldsymbol{f}_f = \frac{1}{1+\delta}\begin{Bmatrix} 0 \\ \dfrac{f}{2D} V_f |V_f| + \dfrac{g}{s_f}\dfrac{\partial h_f}{\partial \xi_f} \end{Bmatrix}, \quad \boldsymbol{f}_b = \frac{1}{1+\delta}\begin{Bmatrix} 0 \\ \dfrac{f}{2D} V_b |V_b| + \dfrac{g}{L_b}\dfrac{\partial h_b}{\partial \xi_b} \end{Bmatrix} \tag{10c}$$

boundary conditions,

$$\begin{cases} P_f(\xi_f = 0, t) = p_{up}, \\ P_f(\xi_f = 1, t) = p_{g0}[(s_{b0} - s_{f0})/(s_b - s_f)]^n, \\ P_b(\xi_b = 0, t) = p_{g0}[(s_{b0} - s_{f0})/(s_b - s_f)]^n, \\ P_b(\xi_b = 1, t) = p_{down} \end{cases} \tag{11}$$

and kinematic conditions,

$$\dot{s}_{\mathrm{f}}(t)=V_{\mathrm{f}}(\xi_{\mathrm{f}}=1,t),\quad \dot{s}_{\mathrm{b}}(t)=V_{\mathrm{b}}(\xi_{\mathrm{b}}=0,t),$$

$$\dot{L}_{\mathrm{b}}(t)=V_{\mathrm{b}}(\xi_{\mathrm{b}}=1,t)-V_{\mathrm{b}}(\xi_{\mathrm{b}}=0,t) \tag{12}$$

where $V_k=V_k(\xi_k,t)\equiv v_k(x(\xi_k,t),t)$, $P_k=P_k(\xi_k,t)\equiv p_k(x(\xi_k,t),t)$. After the coordinate transformation, the motion of the filling fluid is described by $V_{\mathrm{f}}(\xi_{\mathrm{f}},t)$ and $P_{\mathrm{f}}(\xi_{\mathrm{f}},t)$ on the time independent domain, $\xi_{\mathrm{f}}\in[0,1]$, and the blocking fluid motion is described by $V_{\mathrm{b}}(\xi_{\mathrm{b}},t)$ and $P_{\mathrm{b}}(\xi_{\mathrm{b}},t)$ on $\xi_{\mathrm{b}}\in[0,1]$.

2 Method of Solution

The first order PDEs (Eq. (9)) are discretized spatially using the Keller box scheme and the method of lines is employed to reduce the PDEs to a system of ODEs, i.e.,

$$\frac{1}{2}\left[\frac{\mathrm{d}(\boldsymbol{u}_k)_i}{\mathrm{d}t}+\frac{\mathrm{d}(\boldsymbol{u}_k)_{i+1}}{\mathrm{d}t}\right]+\boldsymbol{b}_k(\boldsymbol{u}_k)_{i+\frac{1}{2}}\frac{(\boldsymbol{u}_k)_{i+1}-(\boldsymbol{u}_k)_i}{(\xi_k)_{i+1}-(\xi_k)_i}+$$

$$\boldsymbol{f}_k(\boldsymbol{u}_k)_{i+\frac{1}{2}}=\boldsymbol{0},\quad k=\mathrm{f},\mathrm{b} \tag{13}$$

where the subscripts i, $i+\frac{1}{2}$, and $i+1$ on $\boldsymbol{u}_k$ represent evaluation at $\xi_k=(\xi_k)_i$, $\frac{1}{2}[(\xi_k)_i+(\xi_k)_{i+1}]$, and $(\xi_k)_{i+1}$.

The resulting equations (Eq. (13)) together with kinematic conditions (ODEs) (Eq. (12)) are solved using a backward differentiation formula. The filling and blocking fluid domains are discretized into m_{f} and m_{b} mesh points. At the 1st, m_{f}-th or m_{b}-th mesh points (boundaries), to use characteristics would be advantageous[19] and ensures that information about $\boldsymbol{u}_{\mathrm{f}}$ and $\boldsymbol{u}_{\mathrm{b}}$ at these points can be transmitted into the filling fluid domain ($\xi_{\mathrm{f}}\in[0,1]$) in the direction of characteristics,

$$\left(\frac{\mathrm{d}\xi_{\mathrm{f}}}{\mathrm{d}t}\right)^{+}=-\frac{\dot{s}_{\mathrm{f}}}{s_{\mathrm{f}}}\xi_{\mathrm{f}}+\frac{V_{\mathrm{f}}}{s_{\mathrm{f}}}+\frac{1}{1+\frac{1}{2}\delta-\frac{1}{2}\delta\,\mathrm{sign}(V_{\mathrm{f}})}\frac{a}{s_{\mathrm{f}}} \tag{14}$$

$$\left(\frac{\mathrm{d}\xi_{\mathrm{f}}}{\mathrm{d}t}\right)^{-}=-\frac{\dot{s}_{\mathrm{f}}}{s_{\mathrm{f}}}\xi_{\mathrm{f}}+\frac{V_{\mathrm{f}}}{s_{\mathrm{f}}}-\frac{1}{1+\frac{1}{2}\delta+\frac{1}{2}\delta\,\mathrm{sign}(V_{\mathrm{f}})}\frac{a}{s_{\mathrm{f}}} \tag{15}$$

for $V_{\mathrm{f}}<<a$, and the blocking fluid domain ($\xi_{\mathrm{b}}\in[0,1]$) in the direction of characteristics,

$$\left(\frac{\mathrm{d}\xi_{\mathrm{b}}}{\mathrm{d}t}\right)^{+}=-\frac{\dot{L}_{\mathrm{b}}}{L_{\mathrm{b}}}\xi_{\mathrm{b}}+\frac{\dot{s}_{\mathrm{b}}+V_{\mathrm{b}}}{L_{\mathrm{b}}}+\frac{1}{1+\frac{1}{2}\delta-\frac{1}{2}\delta\,\mathrm{sign}(V_{\mathrm{b}})}\frac{a}{L_{\mathrm{b}}} \tag{16}$$

$$\left(\frac{\mathrm{d}\xi_{\mathrm{b}}}{\mathrm{d}t}\right)^{-}=-\frac{\dot{L}_{\mathrm{b}}}{L_{\mathrm{b}}}\xi_{\mathrm{b}}+\frac{\dot{s}_{\mathrm{b}}+V_{\mathrm{b}}}{L_{\mathrm{b}}}-\frac{1}{1+\frac{1}{2}\delta+\frac{1}{2}\delta\,\mathrm{sign}(V_{\mathrm{b}})}\frac{a}{L_{\mathrm{b}}} \tag{17}$$

for $V_{\mathrm{b}}<<a$.

For the valve-located upstream and the pump being the source of energy, the numerical boundary condition for V_{f} at $\xi_{\mathrm{f}}=0$ is

$$V_{\mathrm{f}}\big|_{\xi_{\mathrm{f}}=0,t=(1+j)\Delta t}=-B_{\mathrm{f}}C_{\mathrm{v}}+\sqrt{(B_{\mathrm{f}}C_{\mathrm{v}})^2-2C_{\mathrm{v}}[C_{\mathrm{f}}-(p_{\mathrm{R}}+p_{\mathrm{c}}+p_{\mathrm{atm}})]} \tag{18}$$

with

$$C_{\mathrm{v}}=\frac{1}{2A+(1+k)\rho},$$

$$C_{\mathrm{f}}=P_{\mathrm{f}}\big|_{\xi_{\mathrm{f}}=0,t=j\Delta t}-V_{\mathrm{f}}\big|_{\xi_{\mathrm{f}}=\zeta,t=j\Delta t}\left(B_{\mathrm{f}}-fD_{\mathrm{f}}\left|V_{\mathrm{f}}\right|\big|_{\xi_{\mathrm{f}}=\zeta,t=j\Delta t}\right)+\frac{gD_{\mathrm{f}}}{s_{\mathrm{f}}\big|_{t=j\Delta t}}\frac{\partial h_{\mathrm{f}}}{\partial\xi_{\mathrm{f}}} \tag{19}$$

$$B_{\mathrm{f}}=\frac{(1+\delta)\rho a}{1+\frac{1}{2}\delta+\frac{1}{2}\delta\,\mathrm{sign}(V_{\mathrm{f}}\big|_{\xi_{\mathrm{f}}=\zeta,t=j\Delta t})},$$

$$D_{\mathrm{f}}=\frac{\rho a\Delta t}{1+\frac{1}{2}\delta+\frac{1}{2}\delta\,\mathrm{sign}(V_{\mathrm{f}}\big|_{\xi_{\mathrm{f}}=\zeta,t=j\Delta t})} \tag{20}$$

$$V_{\mathrm{f}}\big|_{\xi_{\mathrm{f}}=\zeta,t=j\Delta t}=\frac{V_{\mathrm{f}}\big|_{\xi_{\mathrm{f}}=0,t=j\Delta t}+\frac{D_{\mathrm{f}}}{\rho}\frac{V_{\mathrm{f}}\big|_{\xi_{\mathrm{f}}=0,t=j\Delta t}-V_{\mathrm{f}}\big|_{\xi_{\mathrm{f}}=\Delta\xi_{\mathrm{f}},t=j\Delta t}}{\Delta\xi_{\mathrm{f}}}}{1+\theta\frac{V_{\mathrm{f}}\big|_{\xi_{\mathrm{f}}=0,t=j\Delta t}-V_{\mathrm{f}}\big|_{\xi_{\mathrm{f}}=\Delta\xi_{\mathrm{f}},t=j\Delta t}}{s_{\mathrm{f}}\big|_{t=j\Delta t}}} \tag{21}$$

$$P_{\mathrm{p}}\big|_{\xi_{\mathrm{f}}=0,t=(1+j)\Delta t}=p_{\mathrm{c}}-AV_{\mathrm{f}}^2\big|_{\xi_{\mathrm{f}}=0,t=(1+j)\Delta t} \tag{22}$$

where $0\leqslant\zeta\leqslant\Delta\xi_{\mathrm{f}}$; Δt and $\Delta\xi_{\mathrm{f}}$ are the time step and mesh length; $\theta=\Delta t/\Delta\xi_{\mathrm{f}}$; and j is the j-th time step. It is noted that other physical boundary conditions are also applicable here.

In practical case, $\dot{s}_{\mathrm{f}}<<a$, $\dot{s}_{\mathrm{b}}<<a$, and $\dot{L}_{\mathrm{b}}<<a$ since the movement of the filling fluid-entrapped air and the blocking fluid-entrapped air interfaces and the relative movement between the ends of the blocking

liquid column move at far smaller speeds than the wave speed.

3 Numerical Results

Calculations of transient flow in rapidly filling pipelines with entrapped air have been carried out to test the present method. The aim is to validate the model by comparing with other theoretical results given that there are no experimental results, and then to apply it to situations which have not yet previously been investigated. In this analysis, the convergence was achieved upon mesh refinement with a typical computation utilizing 40-mesh points for filling and blocking fluid domains.

Our first example considers a simple undulating elevation pipeline with a centrifugal pump (see Fig. 2), used by Cabrera et al.[20] The pump starts against a closed valve; the valve is opened after the rotational speed of the pump has reached its nominal value. The upstream boundary condition is $p_{\mathrm{f}}(x=0,t)=p_{\mathrm{R}}+p_{\mathrm{p}}+p_{\mathrm{atm}}-\frac{1}{2}(1+k)\rho V_{\mathrm{f}}^2(0,t)$, in which p_{R} is the reservoir pressure and p_{atm} is the atmospheric pressure. The blocking fluid flows downstream with free discharge to the atmosphere; the downstream boundary condition is $p_{\mathrm{b}}(x=s_{\mathrm{b}}+L_{\mathrm{b}},t)=p_{\mathrm{atm}}$. The geometrical and physical parameters are $p_{\mathrm{R}}=5\,\mathrm{m}$, $p_{\mathrm{p}}=\left(165-0.3997\frac{V_{\mathrm{f}}}{\mathrm{m}\cdot\mathrm{s}^{-1}}(x=0,t)\right)\mathrm{m}$, $L_1=500\,\mathrm{m}$, $L_2=1000\,\mathrm{m}$, $s_{\mathrm{f0}}=1\,\mathrm{m}$, initial blocking fluid length $L_{\mathrm{b0}}=735\,\mathrm{m}$, $s_{\mathrm{b0}}=10\,\mathrm{m}$, $D=0.3\,\mathrm{m}$, $f=0.018$, valve loss for open valve $k_0=1$, $\alpha_1=0.1$, $\alpha_2=0.2$, valve loss $k=k_0(t/T)^{-1.6}$ for $0<t<T$ and $k=k_0$ for $t\geqslant T$ in which T is the valve opening time. After the coordinate transformation, the boundary conditions are $P_{\mathrm{f}}(\xi_{\mathrm{f}}=0,t)=p_{\mathrm{R}}+p_{\mathrm{p}}+p_{\mathrm{atm}}-\frac{1}{2}(1+k)\rho V_{\mathrm{f}}^2(\xi_{\mathrm{f}}=0,t)$, $P_{\mathrm{b}}(\xi_{\mathrm{b}}=1,t)=p_{\mathrm{atm}}$. Initial conditions after coordinate transformation are $P_{\mathrm{f}}(\xi_{\mathrm{f}},t=0)=p_{\mathrm{atm}}-\frac{1}{10}\rho g s_{\mathrm{f0}}(1-\xi_{\mathrm{f}})$, $V_{\mathrm{f}}(\xi_{\mathrm{f}},t=0)=0$, $P_{\mathrm{b}}(\xi_{\mathrm{b}},t=0)=p_{\mathrm{atm}}+\frac{1}{10}\rho g L_{\mathrm{b0}}\xi_{\mathrm{b}}$ for $\xi_{\mathrm{b}}\leqslant\frac{500-s_{\mathrm{b0}}}{L_{\mathrm{b0}}}$ or $p_{\mathrm{atm}}+\frac{1}{5}\rho g L_{\mathrm{b0}}(1-\xi_{\mathrm{b}})$ for $\xi_{\mathrm{b}}>\frac{500-s_{\mathrm{b0}}}{L_{\mathrm{b0}}}$, $V_{\mathrm{b}}(\xi_{\mathrm{b}},t=0)=0$, $s_{\mathrm{f}}(t=0)=s_{\mathrm{f0}}$, and $s_{\mathrm{b}}(t=0)=s_{\mathrm{b0}}$.

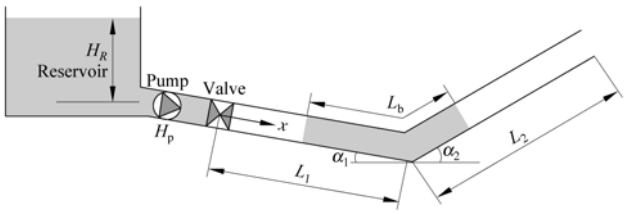

Fig. 2 Diagram of a pipeline with an entrapped air pocket

Figure 3 shows the maximum entrapped air pressure and filling fluid front velocity obtained using MOL, compared with the results obtained using the model based on MOC[18] and a lumped parameter model[6]. It can be seen that the lumped parameter model underestimates the peak velocities of filling fluid at $x=s_{\mathrm{f}}$, $V_{\mathrm{f}}^{\max}(x=s_{\mathrm{f}},t)$, and overestimates the maximum pressures of entrapped air, $p_{\mathrm{g}}^{\max}$, compared with the present model and the previous MOC model. This is due to the fact that $\partial h_k/\partial x$ is averaged for the whole

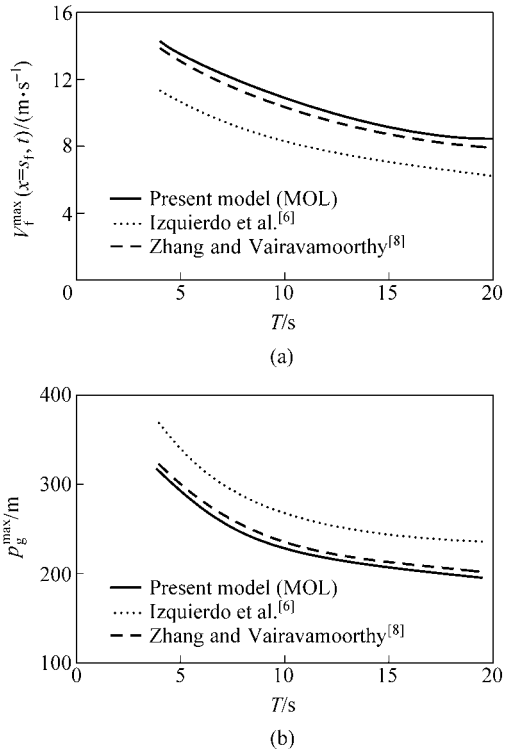

Fig. 3 Comparison of the present model with the previous models: (a) Variation of maximum front velocity of filling fluid ($V_{\mathrm{f}}^{\max}(x=s_{\mathrm{f}},t)$) with valve opening time (T); (b) Variation of maximum pressure of entrapped air ($p_{\mathrm{g}}^{\max}$) with T

filling/blocking fluid domain in the lumped parameter model. Furthermore, convective terms and transient wall shear stress are neglected in the lumped parameter model. It is noted that the proposed model agrees well with the MOC model. Maximum pressures and velocities decrease with increasing valve opening time, as expected.

Figue 4 shows the evolution of flow velocities and pressure for valve opening time $T = 5, 10,$ and 20 s. The amplitudes of filling and blocking fluid velocity and gas pressure pulsation decay with increasing T, and that their periods increase with increasing T.

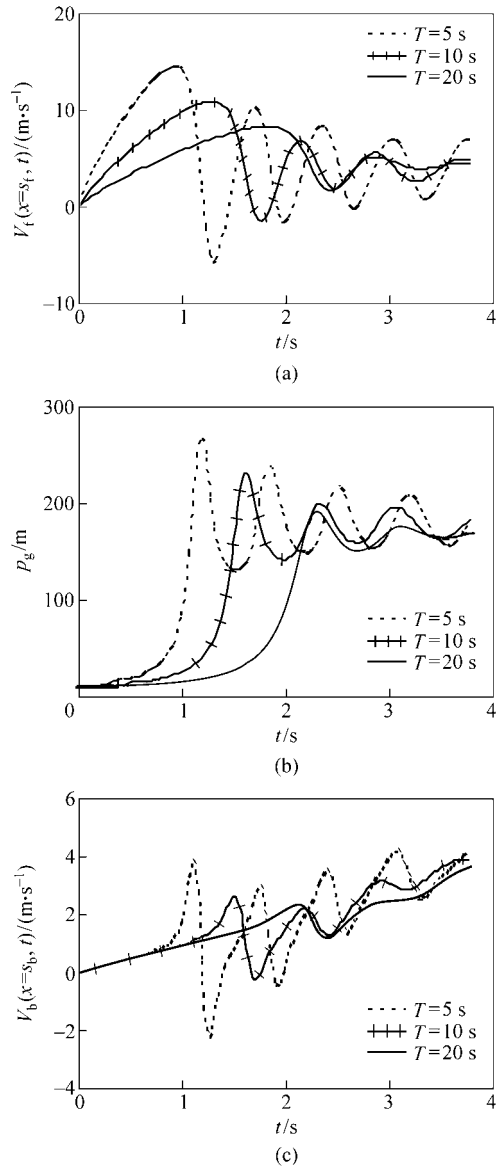

Fig. 4 Evolution of fluid flow for T=5, 10, 20 s: (a) Variation of filling fluid front velocity with time; (b) Variation of entrapped air pressure with time; (c) Variation of blocking fluid flow velocity at x=s_b

Given the validation of the present model, the next example is to assess potential risks of entrapped air in terms of maximum pressure and velocity at various entrapped air pocket sizes. In this example, we consider a pipeline system with the same parameters as the previous one except $T = 20$ s and varying entrapped air pocket length L_{g0} and its consequent variation in blocking fluid length, L_{b0}, in which $L_{b0} = \frac{3}{2}\left(500\text{ m} - s_{f0} - L_{g0}\right)$.

Figure 5 shows the variation of fluid flow with entrapped air pocket size at $T = 20$ s. Maximum flow velocities at $x = s_f$ ($V_f^{max}(x = s_f, t)$) increase slowly for a smaller L_{g0} (i.e., $L_{g0} < 20$ m) and then significantly for a larger L_{g0} (i.e., $L_{g0} > 20$ m), and eventually tend to be steady, as shown in Fig. 5a. Figure 5b shows that the trend in the variation of the maximum entrapped air pressure (p_g^{max}) with L_{g0} is different from that generally presented in the literatures[6]. The previous results revealed that to increase L_{g0} results in monotonously decreasing p_g^{max}, whereas the present results indicate that there are three phases in the

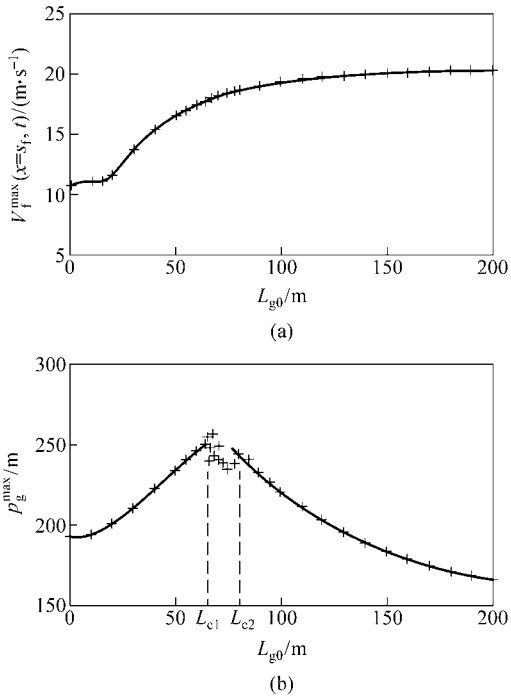

Fig. 5 Variation of fluid flow with entrapped air pocket size at T=20 s in which $L_{b0} = \frac{3}{2}(500\text{ m} - s_{f0} - L_{g0})$.

variation of p_g^{max} with: (1) for $L_{g0} \leqslant L_{c1}$ (i.e., $L_{c1} = 65$ m) in which L_{c1} is the first critical initial entrapped air pocket length, p_g^{max} increases with increasing L_{g0}; (2) for $L_{c1} \leqslant L_{g0} \leqslant L_{c2}$ in which L_{c2} is the second critical initial entrapped air pocket length, p_g^{max} appears to pulse with L_{g0}; and (3) for $L_{g0} \geqslant L_{c2}$ (i.e., $L_{c2} = 80$ m), p_g^{max} decreases with increasing L_{g0}. The difference between the present study and the previous work[6] can probably be attributed to the fact that the previous study is confined to the third phase only. It should be noted that the present results are obtained from the solution of the governing equations (Eq. (9)), and further work is required to verify these results through experimental work.

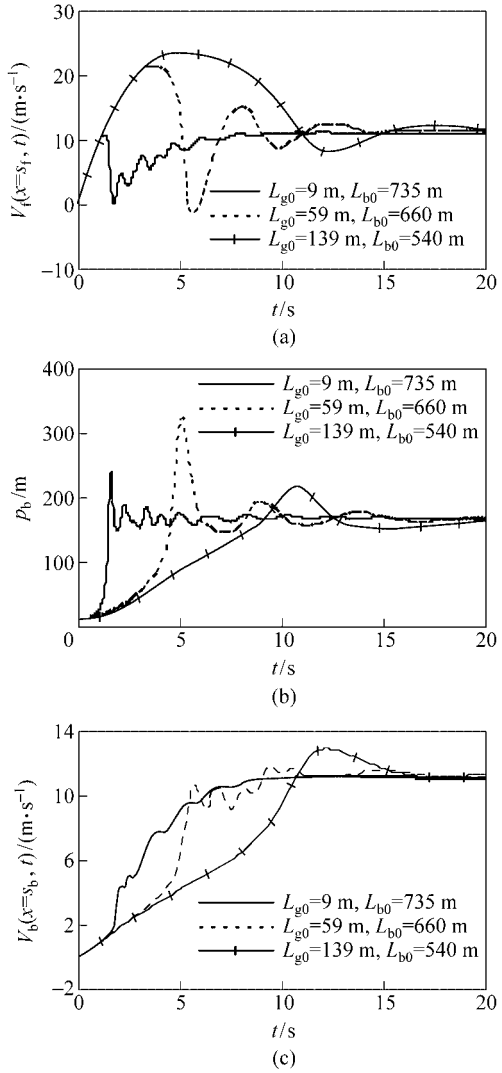

Fig. 6 Evolution of fluid flow for different entrapped air pocket sizes at *T*=10 s: (a) Variation of filling fluid front velocity with time; (b) Variation of entrapped air pressure with time; (c) Variation of blocking fluid flow velocity at $x=s_b$

Figure 6 shows the evolution of entrapped air pressure, filling fluid velocity at $x = s_f$ and blocking fluid velocity at $x = s_b$ for $L_{g0} = 9$, 59, and 139 m ($L_{b0} = 735$, 660, and 540 m), respectively. Pulsation frequency of flow velocity and pressure decreases with increasing L_{g0} (accordingly decreasing L_{b0}). For a larger L_{g0}, velocity and pressure waves dissipate faster due to a larger cushion effect. The entrapped air pressure and filling fluid front velocity peak earlier with decreasing L_{g0}. After about 20 s, the waves of pressure and velocity tend to be steady.

4 Conclusions

In this paper, a mathematical model is presented for the charging-up process in a pipeline with one entrapped air pocket. The method is based on the water hammer equations and uniform gas compression equation. These equations in time-varying computational domains are solved utilizing a coordinate transformation technique and MOL. The good agreement between MOL and MOC shows that the present numerical model offers an alternative way to investigate the behavior of the charging-up process in pipelines with entrapped air.

Comparison of present theoretical results with theoretical results obtained using a lumped-parameter model demonstrates that ignoring elastic effects and transient shear stresses leads to overestimating maximum gas pressures (p_g^{max}) and underestimating filling fluid front velocities. Results also revealed that there are three phases in the variation of p_g^{max} with initial entrapped air pocket length (L_{g0}): (1) for $L_{g0} \leqslant L_{c1}$, p_g^{max} increases with increasing L_{g0}, (2) for $L_{c1} \leqslant L_{g0} \leqslant L_{c2}$, p_g^{max} pulsates with L_{g0}, and (3) for $L_{g0} \geqslant L_{c2}$, p_g^{max} decreases with increasing L_{g0} in which $L_{c1} = 65$ m and $L_{c2} = 80$ m in the examined case.

To minimize gas pressure in the pipeline, the initial size of an entrapped air pocket should not be allowed to naturally develop to a critical amount, and this could

be achieved by shortening the interruption of service or by installing air release valves. Lengthening valve opening time will reduce the peak pressures. The longer the valve opening time, the lower the maximum pressure of the entrapped air pressure.

Finally, the present study is confined to modelling transient flow in a filling pipeline with one entrapped air pocket. Modelling results for only one air pocket generally reflect the main feature of transient flow in the term of peak pressure as the previous findings demonstrate that the presence of two or more entrapped air pockets does not significantly influence the maximum pressure of the first air pocket[6]. An undulating pipeline system may have several air pockets each admitted at high points of the pipeline. The present method could also be useful to model the pipeline system with several entrapped air pockets.

References

[1] Vairavamoorthy K, Lin Z, Zhang Y L. Water networks in developing countries: Modelling the pipe charging process. To appear in *J. Hydr. Res*., 2006.

[2] Chaiko M A, Brinckman K W. Models for analysis of water hammer in piping with entrapped air. *J. Fluids Engrg. ASME*, 2002, **124**: 194-204.

[3] Martin C S. Entrapped air in pipelines. In: Proc. 2nd Int. Conf. Pressure Surges. London, 1976: 15-28.

[4] Cabrera E, Abreu J, Perez R, Vela A. Influence of liquid length variation in hydraulic transients. *J. Hydr. Engrg., ASCE*, 1992, **118**(12): 1639-1650.

[5] Liou C P, Hunt W A. Filling of pipelines with undulating elevation profiles. *J. Hydr. Engrg., ASCE*, 1996, **122**(10): 534-539.

[6] Izquierdo J, Fuertes V S, Cabrera E, Iglesias P L, Garcia-Serra J. Pipelines start-up with entrapped air. *J. Hydr. Res.*, 1999, **37**(5): 579-590.

[7] Zhou F, Hicks F E, Steffler P M. Transient flow in a rapidly filling horizontal pipe containing trapped air. *J. Hydr. Engrg.*, 2002, **128**(6): 625-634.

[8] Zhang Y L, Vairavamoorthy K. Transient flow in rapidly filling air-entrapped pipelines with moving boundaries. *Tsinghua Science and Technology*, 2006, **11**(3): 313-323.

[9] Suwan K, Anderson A. Method of lines applied to hyperbolic fluid transient equations. *Int. J. Numer. Meth. Engrg.*, 1992, **33**: 1501-1511.

[10] Zhang Y L, Matar O K, Craster R V. Surfactant spreading on a thin weakly viscoelastic film. *J. Non-Newton. Fluid Mech.*, 2002, **105**(1): 53-78.

[11] Zhang Y L, Matar O K, Craster R V. Analysis of tear film rupture: Effect of mucus rheology. *J.Colloid Interf. Sci.*, 2003, **262**(1): 130-148.

[12] Selcuk N, Tarhan T, Tanrikulu S. Comparison of method of lines and finite difference solutions of 2-D Navier-Stokes equations for transient laminar pipe flow. *Int. J. Numer. Meth. Engrg.*, 2002, **53**: 1615-1628.

[13] Zhang Y L, Vairavamoorthy K. Analysis of transient flow in pipelines with fluid-structure interaction using method of lines. *Int. J. Numer. Meth. Engrg.*, 2005, **63**(10): 1446-1460.

[14] Streeter V L, Wylie E B. Fluid Mechanics, 6th Edition. New York: McGraw-Hill Book Co., 1975.

[15] Bergant A, Simpson A R. Estimating unsteady friction in transient cavitating pipe flow. In: Proc. 2nd Int. Conf. on Water Pipelines Sys., BHR Group, Edinburgh, UK, 1994: 333-342.

[16] Brunone B, Golia U M, Greco M. Some remarks on the momentum equation for fast transients. In: Int. Meeting on Hydraulic Transients with Column Separation, 9th Round Table, IAHR, Valencia, Spain, 1991: 140-148.

[17] Vitkovsky J, Lambert M, Simpson A, and Bergant A. Advances in unsteady friction modelling in transient pipe flow. In: Anderson A, ed. Pressure Surges, Safe Design and Operation of Industrial Pipe Systems. England: Professional Engineering Publishing Ltd., 2000: 471-482.

[18] Bergant A, Simpson A R, Vitkovsky J. Development in unsteady pipe flow friction modelling. *J. Hydr. Research*, 2001, **39**(3): 249-257.

[19] Pennington S V, Berzins M. New NAG library software for first-order partial differential equations. *ACM T. Math. Software*, 1994, **20**(1): 63-99.

[20] Cabrera E, Izquierdo J, Abreu J, Iglesias P L. Filling of pipelines with undulating elevation profiles—Discussion. *J. Hydr. Engrg. ASCE*, 1997, **123**(12): 1170-1173.